Iraqi Journal of Physics, 2019 *Vol.17, No.41, PP. 15-28*
DOI: 10.20723/ijp.17.41.15-28

Effect of thickness on structural properties of $Bi_xSb_{2-x}Te_3$ thin films

Hussain. M. Selman and Salma M. Shaban

Department of Physics, College of Science, University of Baghdad, Iraq

E-mail: husshdeaaee@gmail.com

Abstract

$Bi_xSb_{2-x}Te_3$ alloys with different ratios of Bi (x=0, 0.1, 0.3, 0.5, and 2) have been prepared, Thin films of these alloys were prepared using thermal evaporation method under vacuum of 10^{-5} Torr on glass substrates at room temperature with different deposition rate (0.16, 0.5, 0.83) nm/sec for thickness (100, 300, 500) respectively. The X–ray diffraction measurements for $Bi_xSb_{2-x}Te_3$ bulk and thin films indicate the polycrystalline structure with a strong intensity of peak of plane (015) preferred orientation with additional peaks, (0015) and (1010) reflections planes, which is meaning that all films present a very good texture along the (015) plane axis at different intensities for each thin film for different thickness. AFM measurements for the thin films of $Bi_xSb_{2-x}Te_3$, show that the grain size and the average surface roughness decreases with increasing of the percentage Bi for different thickness.

Key words
Bismuth tellurium, antimony tellurium, alloys, thin films, thermal evaporation, structural properties.

Article info.
Received: Sep. 2018
Accepted: Nov. 2018
Published: Jun. 2019

تاثير السمك على الخصائص التركيبية لسبائك وأغشية $Bi_xSb_{2-x}Te_3$ الرقيقة

حسين محمد سلمان و سلمى مهدي شعبان

قسم الفيزياء، كلية العلوم، جامعة بغداد

الخلاصة

حضرت سبائك ($Bi_xSb_{2-x}Te_3$) بنسب مختلفة من محتوى Bi, (x=0, 0.1, 0.3, 0.5, 2) وحضرت الاغشية الرقيقة لهذه السبائك باستخدام تقنية التبخير الحراري على قواعد من مادة الزجاج وعند ضغط واطئ (10^{-5}) تور عند درجة حرارة الغرفة وبمعدل ترسيب (0.16, 0.5, 0.83) نانومتر بالثانية للسمك (100, 300, 500) نانومتر على التوالي. اظهرت فحوصات حيود الاشعة السينية لسبائك واغشية $Bi_xSb_{2-x}Te_3$ بانها تمتلك تركيب متعدد التبلور، مع التوجيه القوي الشدة للسطح (015). لوحظ أن هناك قمم حيود اضافية، تتوافق مع الانعكاسات عن السطوح البلورية، (1010) و (0015)، وهذا يعني أن جميع الأغشية ذات تركيب جيدعلى طول المستوى (015) بشدات مختلفة لكل غشاء رقيق. اظهرت قياسات AFM للاغشية الرقيقة $Bi_xSb_{2-x}Te_3$ نقصان حجم الحبيبة ومتوسط خشونة السطح مع زيادة للنسبة المئوية ل Bi ولمختلف قيم السمك.

Introduction

many researchers recently resorted to study and expand both of clean and renewable energies, and tended to lessens the credence for energy that is produced from fossilized fuels (e.g. gas, oil, petroleum and coal etc), and also because of negatively effect of the surrounding environment to this type fuel and in turnby human, therefore the most frequent type of energy that researchers had been concerned since 1950. The energy that was producing by thermoelectric devices, these materials are able to make the thermal energy for direct conversion into electrical energy and vice versa [1]. Than in depending on the temperature process, so the thermoelectric materials can be classified to: Materials with high temperature above (900) K, as (SiGe) alloys, materials with mid-range temperature, as (PbTe) alloys, and materials with low temperature, as

(Bi_2Te_3) and (Sb_2Te_3) based alloys for application at room temperature that belong for (V-VI) group [2].

In 1954 Goldsmid demonstrated the excellent thermoelectric properties of Bismuth Telluride, attributed mainly to the large mean molecular mass, low melting temperature and partial degeneracy of the conduction and valence bands of this V-VI chalcogenide [2]. Since that, bismuth telluride has been widely studied as a thermoelectric material with a narrow band gap, particularly in the temperature range around 300 K [2, 3]. Bi_2Te_3 or Sb_2Te_3 has a rombohedral structure with space group R3m, and the lattice is stacked in a repeated sequence of five atom layers: Te_1-Bi-Te_2-Bi-Te_1 along the c-axis, Te or and (Sb) and Bi layers are held together by strong ionic-covalent bonds (Te_1 or\ and Sb_1-Bi and Bi-Te_2 or \and Sb_2), while The Te1 or\and Sb1 bonds between cells are of the Van der Walls type and are extremely weak [4, 5]. Bismuth telluride compounds can be doped as either n- or p-type material by creating either a tellurium-rich composition or a bismuth-rich composition respectively [6].

In (2006) P.G.Ganesan et al have study thin films $(Bi_{0.5}Sb_{0.5})_2Te_3$ for different thickness which deposited on a glass substrate by flash evaporation method in a vacuum $1*10^{-5}$ Torr. X-ray diffraction and Transmissin electron microscopic TEM analysis show that these films are polycrystalline even in the as-deposited state and the post-deposition annealing leads to grain growth. Electrical resistivity studies were carried out on these films as a function of T (300–450) k and film thickness (450–2000) A° [7]. In (2010) Pradyumnan et al have studied the Bi_2Te_3, Sb_2Te_3 and Bi_2Te_3, Sb_2Te_3 bilayer thin films various thickness which prepared by thermal evaporation method [8]. X-ray is use for the properties of the samples. Electrical studies is carried out using standard four probe method also the activation energy of each films. Thermoelectric behavior of each sample is determinedat different temperature regions [8].

In (2015) Das et al. have study Bismuth Telluride films (Bi_2Te_3) were prepared using thermal evaporation technique in a vacuum 10^{-5} Torr on the glass substrate [9]. The study of electrical characterizations of Bi_2Te_3 thin films was carried out in the different thickness about 50-300 nm and temperature range 300-470 K. The electrical conductivity was found to increase with thickness of the films and temperatures. The activation energy was decreased with film thickness while the grain size was increased with the thickness. The Hall co-efficient, carrier mobility, carrier concentration, also studied. These results suggest that the investigated films are semiconducting in nature [9]. In (2018) A. M. ADAM et al have study Micro/ Nano-powders of the chalcogenide $(Sb_{1-x}\ Bi_x)_2Te_3$ system were composed by ball milling technique. The prepared powders were used as a source to production thin films with the aid of vacuum thermal evaporation methods. Crystal structure of the powders was studied by using XRD and SEM techniques, while the grown films were investigated via SEM and AFM analysis, which leads to an increased electrical conductivity and a reduced to the electronic thermal conductivity and the Seebeck coefficient [10].

The aim of this study is to produce thermoelectric $Bi_xSb_{2-x}Te_3$ thin films using thermal evaporation technique, and look into the effectiveness of Bi percentage on the structural properties, in order to use it in the future to make thermoelectric devices, which were very effective to provide a clean

renewable energies to ensure a clean surrounding environment.

Experimental

To study the nano or micro structural properties of materials (Bulk or thin films), the X-ray diffraction technique (XRD) was used for this purpose. The reason of using X-ray diffraction (XRD) is attributed to a wavelength which is close to the distance between lattice points. The principle work of this technique depends on "Bragg law" which said the difference in the path between two beams is equal to the multiplying of the wavelength, and is given by Eq. (1) [11]:

$$n\lambda = 2d\ sin\theta \quad (1)$$

where: n is integer representing the rank of overlap, ɵ is Bragg angle, λ is wavelength.

The X-ray diffraction mode of amorphous materials appears as interfering and central wide halos, the sharp rings shaping points to the polycrystalline materials and the spots form show to a single crystalline materials. The peaks site offer information about structure and lattice orientation, the peaks width expounds the grain size of the crystals that were formed in the materials [12-14]. By using Scherer's formula we can calculated the grain size from XRD test as shown in Eq.(2) [15].

$$G.S = \frac{0.9\lambda}{\beta_{FWHM} cos\theta} \quad (2)$$

where: β_{FWHM} is Full Width at Half Maximum (FWHM).

To prepare the $Bi_xSb_{2-x}Te_3$ alloy with x = (0, 0.1, 0.3, 0.5, 2), in the beginning we have raw materials as powder. These materials are (Bi with purity 99.9, Sb purity 99.6, and Te purity 99.98) powders. All elements' weight in the alloy is obtain by a highly sensitive and precise balance and depended on the atomic weight, atomic mass, density of each element and the ratio of the alloys. The weight of each alloy is 3.5 g, the powders are mixed together and then located in a clean and dry quartz ampoules, then sealed under vacuum ($1*10^{-3}$) Torr using a diffusing pump, after they are placed in a thermal oven at (900 ^oC) for 7 hr till they become homogeneous alloy at room temperature.

(CuKα) radiation of wavelength (1.541A°), Current (30 mA), Voltage (40kV), Range (20000) counts/s, 10-80 (deg); Scan Mode: continuous scan, scanning speed: (5 deg /min). The Bragg's condition for the diffraction can be show by the Eq.(1)

To determine the surface of the prepared $Bi_x\ Sb_{2-x}Te_3$ thin film in nanoscale which can be measured using Atomic Force Microscope (AFM). To study and draw the surface topography we used this device in the field of nanotechnology; this microscope has the capability of analyzing up parts of a nanometer, this device exceeds the limit magnification optical microscopes more than (1000) times. In this study we used (AFM) system is (AA3000) type.

Results & discussion

The Results of the experimental investigations of $Bi_xSb_{2-\ x}Te_3$ alloys and thin films are interducing in this section. That structural measurements as : X-Ray Diffraction (XRD), Atomic Force Microscopy (AFM) of $Bi_xSb_{2-\ x}Te_3$ alloys and thin films. The elements' concentration of Bi, Sb, and Te in the alloy of deferent values of x = (0, 0.1, 0.3, 0.5 and 2) have been determined by X-Ray fluorescence spectroscopy (XRF), it can be noticed that the compositional analysis of these alloys are in good stoichiometric percentage compared with the theoretical atomic percentages as show in Table 1.

Table 1: The theoretical and experimental atomic percentage of ($Bi_x Sb_{2-x}Te_3$) alloys.

Alloys	Elements	Atomic percentage %	
		Theoretical	Experimental
Sb_2Te_3	Sb	40	41.6
	Te	60	58.4
$Bi_{0.1}Sb_{1.9}Te_3$	Bi	4	5.09
	Sb	36	35.18
	Te	60	59.73
$Bi_{0.3}Sb_{1.7}Te_3$	Bi	12	12.41
	Sb	28	28.17
	Te	60	59.42
$Bi_{0.5}Sb_{1.5}Te_3$	Bi	15	16.25
	Sb	25	24.33
	Te	60	59.42
Bi_2Te_3	Bi	40	41.11
	Te	60	58.89

Fig.1 shows the XRD patterns of $Bi_x Sb_{2-x}Te_3$ alloys at different Bi ratio (x=0, 0.1, 0.3, 0.5, and 2). It can be noticed that all samples have a polycrystalline structure with main diffraction peak to all alloys at (015) and the additional peaks; (0015), (006) and (1010), as see in Table 2. These reflections' position have been compared with standard (JCPDS). From the results the most defraction peak appeared at (015) was shiftid towareds smaller 2Θ with increasing of Bi percentage, due to decrease in strain in the structure which happened because of Bi incoperation with lattice sites of Sb these results agrees with Tan [16].

Figs. 2-4 shows the XRD patterns of $Bi_xSb_{2-x}Te_3$ thin films which deposited by thermal evaporation method at room temperature with different of (Bi) ratio of x= (0, 0.1, 0.3, 0.5, and 2) and different thickness (100 nm, 300 nm, and 500 nm). From these figures we noticed that all thin films have a polycrystalline structure, also we observed that a main preferred peak is (015), which shifted towards the smaller 2Θ with increasing in Bi percentage, this behavior is attributed to the change in crystalline of the samples, which agreed with Sánchez [17] and Zhang [18]. As well as it can be noticed from the figure additional peaks which were corresponding to surface reflections planes (1010) and (101). The data of measuring (XRD) were approximately close to that listed in (JCPDS 96-7591) standards. All The results are listed in Table 3.

The values of crystallite size of $Bi_xSb_{2-x}Te_3$ thin films were calculated from measuring the half width of the peak maximum intensity FWHM, and 2θ of the directions' peaks by using Scherer's formula Eq.(2), [15] The grain size of $Bi_x Sb_{2-x}Te_3$ thin films, decreases with increasing of the Bi percentage for all thickness as shown in Table3, the grain size for various peaks of x-ray diffraction decreases when x value increases and this can be attributed to additive of Bi atoms in the structure of Sb_2Te_3 due to the different in atoms radius for Bi (1.6Å) and Sb (1.45 Å). This result is agree with Song [19] and Das [20].

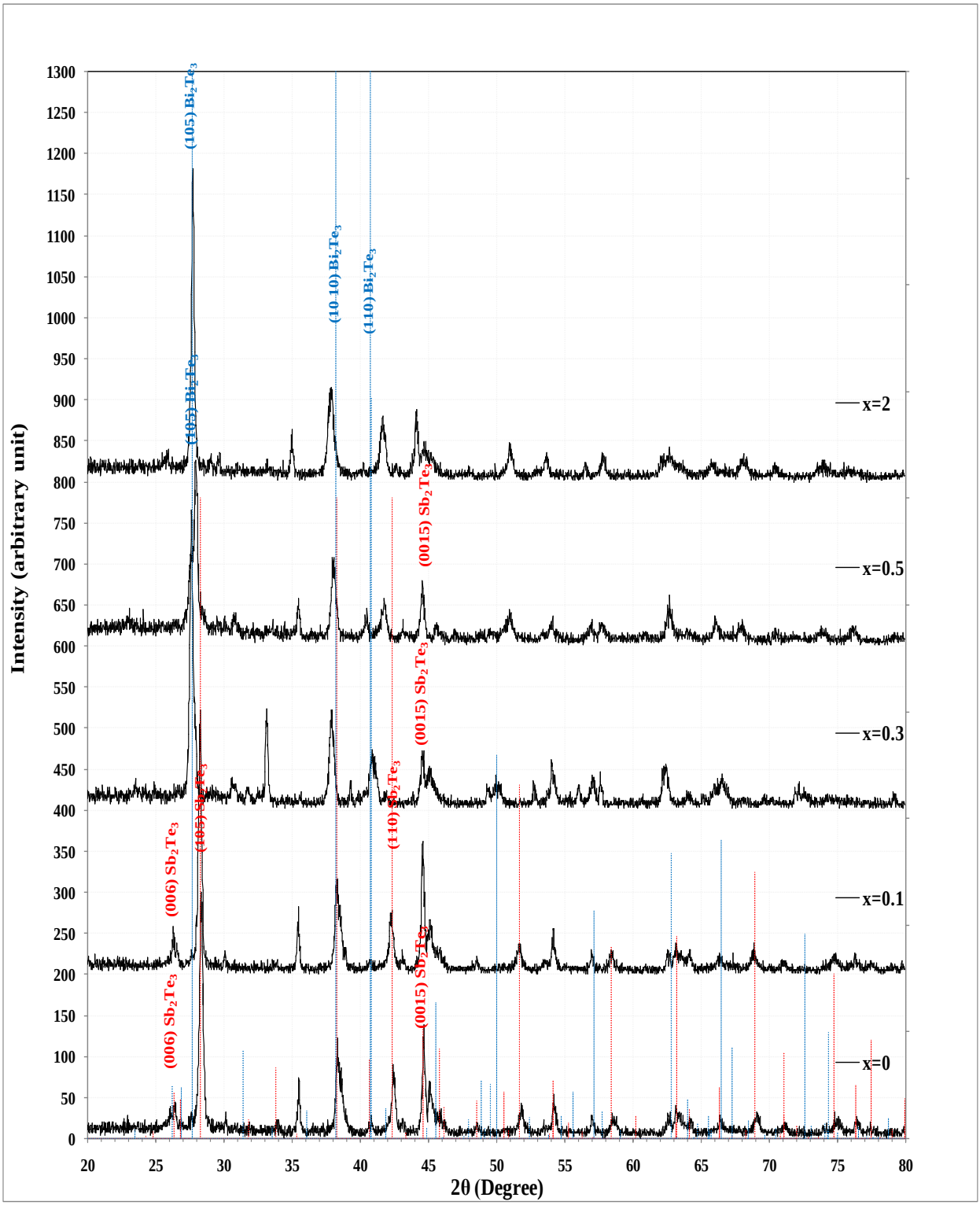

Fig.1: XRD pattern for $Bi_xSb_{2-x}Te_3$ alloys at different ratio of Bi(0, 0.1, 0.3, 0.5, and 2).

Table 2: The calculated values of interplaner distance(d-values), 2Θ, G.S, and hkl for the $Bi_xSb_{2-x}Te_3$ alloys.

X	(hkl)	2Θ(exp) (deg.)	d stand.(A)	d Exp.(°A)	G.S (nm)	Aver. G.S(nm)	I/I_0 (a.u)
0	015	28.33	3.157	3.146	31.87	30.33	100%
	0015	44.65	2.030	2.027	27.18		35%
	1010	38.35	2.356	2.349	31.94		43%
0.1	015	28.25	3.171	3.156	28.70	30.12	100%
	0015	44.58	2.032	2.030	31.91		53%
	1010	38.25	2.356	2.350	29.76		35%
0.3	015	28.22	3.171	3.154	27.00	27.88	100%
	0015	44.41	2.032	2.341	30.60		28%
	1010	38.19	2.356	2.354	26.06		23%
0.5	015	27.93	3.171	3.191	25.69	23.81	100%
	0015	44.30	2.032	2.031	22.20		44%
	1010	38.03	2.356	2.363	23.56		44%
2	015	27.62	3.230	3.226	28.75	29.11	100%
	0015	44.35	1.996	2.019	31.19		31%
	1010	37.89	2.360	2.372	27.39		31%

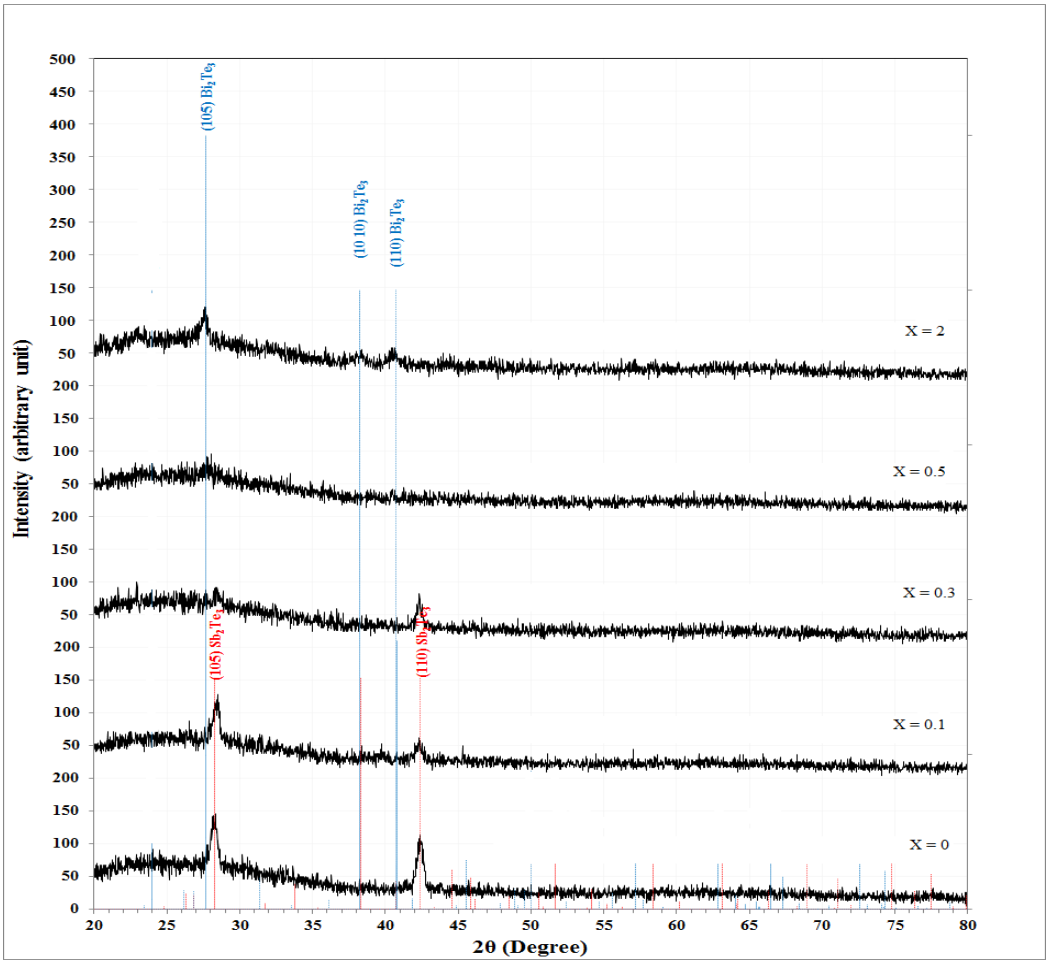

Fig.2: XRD patterns of $Bi_x Sb_{2-x}Te_3$ thin films with different Bi content with (x=0, 0.1, 0.3, 0.5, and 2) at thickness (100 nm).

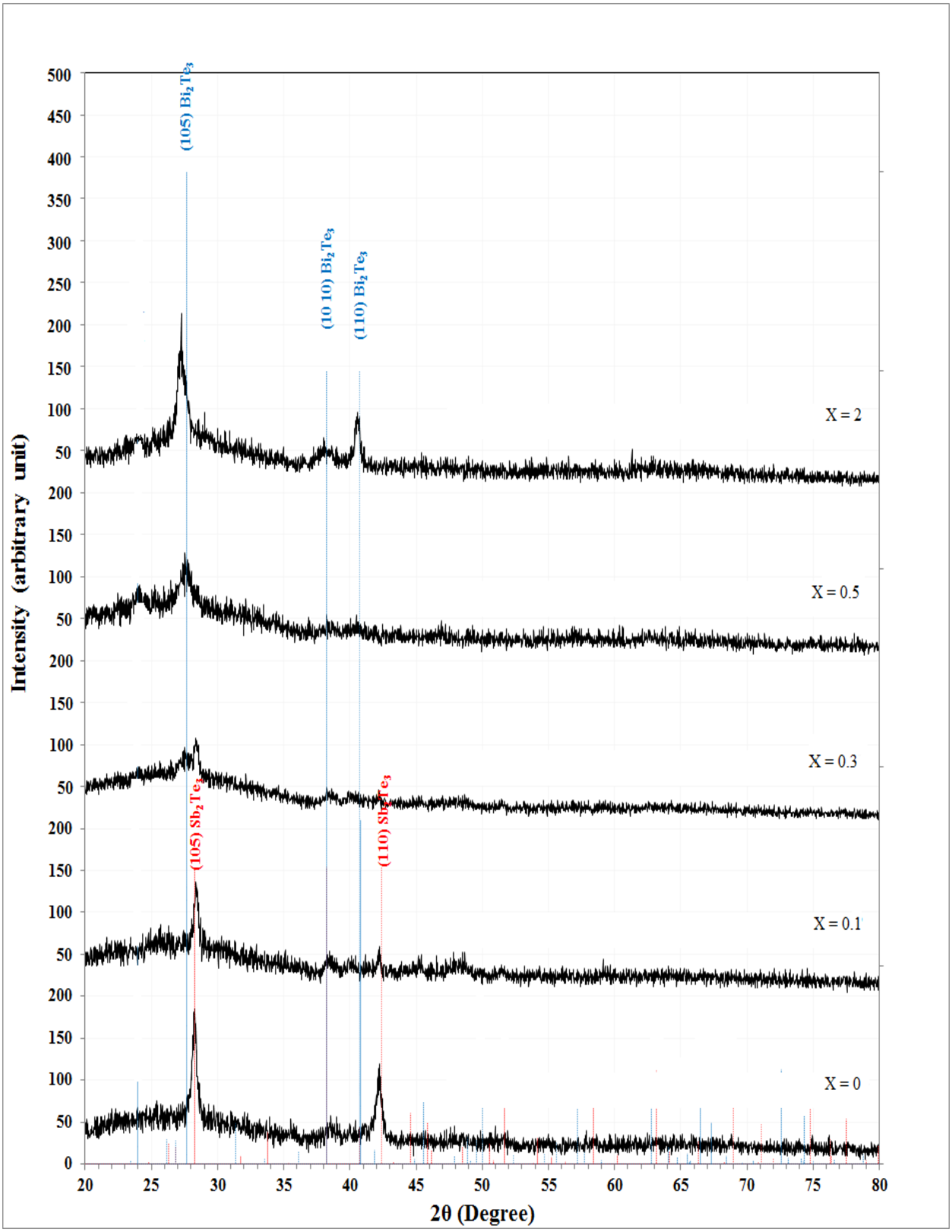

Fig.3: XRD patterns of $Bi_x Sb_{2-x}Te_3$ thin films with differentBi content with (x=0, 0.1, 0.3, 0.5, and 2) at thickness (300 nm).

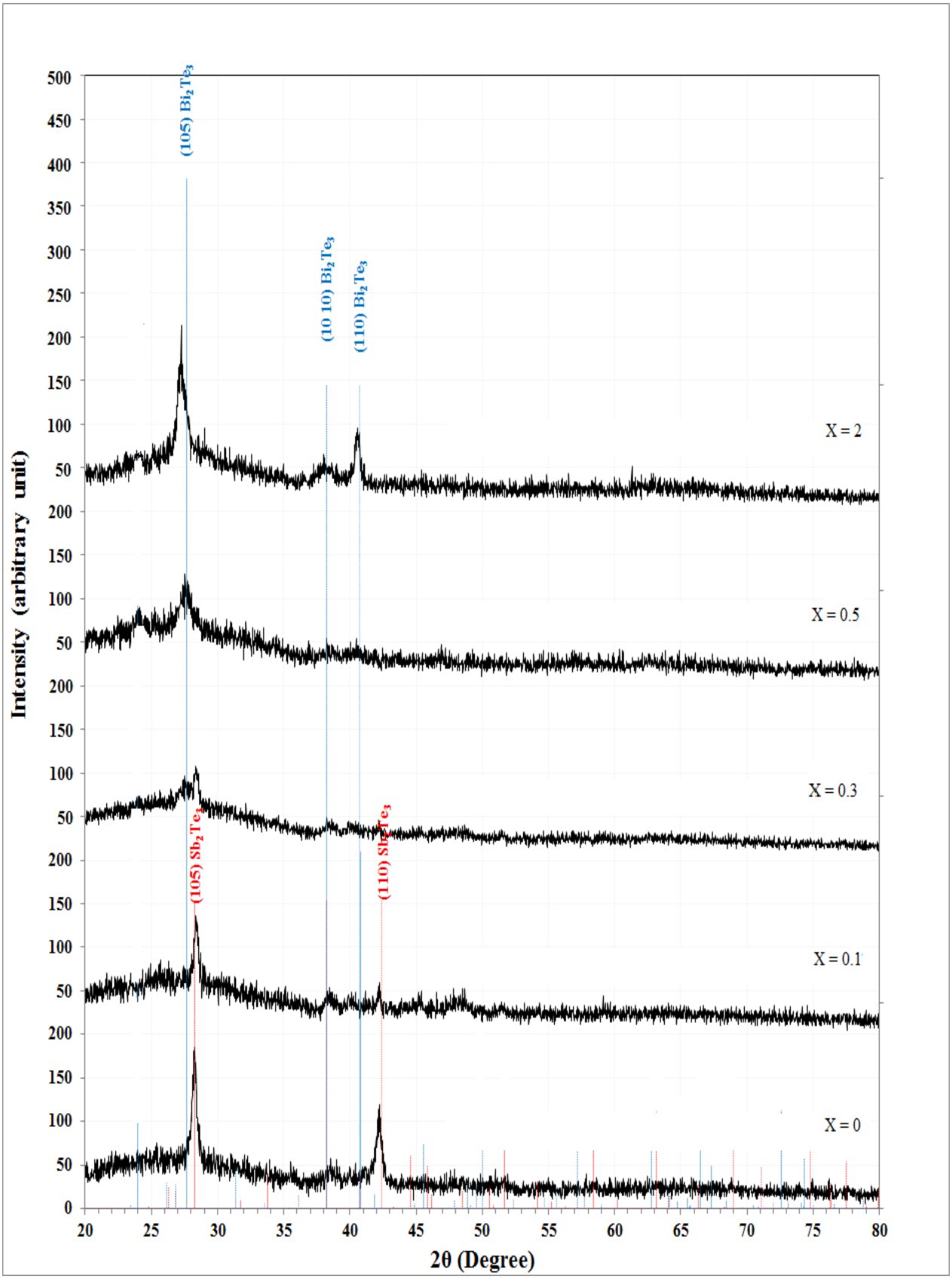

Fig.4: XRD patterns of $Bi_x Sb_{2-x}Te_3$ thin films with different Bi content with (x=0, 0.1, 0.3, 0.5, and 2) at thickness (500 nm).

Table 3: The calculated values of (d-values), 2Θ, G.S, and hkl for $Bi_x Sb_{2-x}Te_3$ thin films at different thickness (100, 300 and 500 nm).

Thickness T(nm)	X	2θ (Deg.)	d_{hkl} Exp.(Å)	d_{hkl} Std.(Å)	Phase	hkl	G.S (nm)	Average G.S(nm)
100	0	28.181	3.1640	3.1578	Hex.Sb_2Te_3	(105)	15.8	14.85
		42.382	2.1310	2.1320	Hex.Sb_2Te_3	(110)	13.9	
	0.1	28.463	3.1332	3.1578	Hex.Sb_2Te_3	(105)	15.8	14.35
		42.288	2.1355	2.1320	Hex.Sb_2Te_3	(110)	12.9	
	0.3	28.322	3.1485	3.1578	Hex.Sb_2Te_3	(105)	12.7	13.40
		42.335	2.1332	2.1320	Hex.Sb_2Te_3	(110)	14.1	
	0.5	27.805	3.2059	3.6925	Hex.Bi_2Te_3	(105)	8.7	8.7
	2	27.570	3.2327	3.2274	Hex.Bi_2Te_3	(105)	13.4	10.6
		38.197	2.3542	2.3773	Hex.Bi_2Te_3	(1010)	9.4	
		40.689	2.2156	2.1975	Hex.Bi_2Te_3	(110)	9.0	
300	0	28.265	3.1548	3.1578	Hex.Sb_2Te_3	(105)	17.8	17.1
		42.215	2.1390	2.1320	Hex.Sb_2Te_3	(110)	16.4	
	0.1	28.396	3.1405	3.1578	Hex.Sb_2Te_3	(105)	17.7	16.15
		42.259	2.1369	2.1320	Hex.Sb_2Te_3	(110)	14.6	
	0.3	28.354	3.1451	3.1578	Hex.Sb_2Te_3	(105)	16.8	14.25
		38.307	2.3477	2.3773	Hex.Bi_2Te_3	(1010)	11.7	
	0.5	27.478	3.2434	3.2274	Hex.Bi_2Te_3	(105)	9.5	9.5
	2	27.259	3.2689	3.2274	Hex.Bi_2Te_3	(105)	10.4	11.5
		38.192	2.3545	2.3773	Hex.Bi_2Te_3	(1010)	9.2	
		40.597	2.2204	2.1975	Hex.Bi_2Te_3	(110)	14.9	
500	0	28.260	3.1554	3.1578	Hex.Sb_2Te_3	(105)	18.3	18.45
		42.420	2.1291	2.1320	Hex.Sb_2Te_3	(110)	19.6	
	0.1	28.260	3.1554	3.1578	Hex.Sb_2Te_3	(105)	17.6	17.65
		42.420	2.1291	2.1320	Hex.Sb_2Te_3	(110)	17.7	
	0.3	27.579	3.2317	3.2274	Hex.Bi_2Te_3	(105)	14.4	15.05
		40.559	2.2224	2.1975	Hex.Bi_2Te_3	(110)	15.7	
	0.5	27.397	3.2527	3.2274	Hex.Bi_2Te_3	(105)	9.0	11.06
		38.199	2.3541	2.3773	Hex.Bi_2Te_3	(1010)	10.9	
		40.650	2.2177	2.1975	Hex.Bi_2Te_3	(110)	13.3	
	2	27.352	3.2580	3.2274	Hex.Bi_2Te_3	(105)	12.0	11.73
		38.108	2.3595	2.3773	Hex.Bi_2Te_3	(1010)	8.8	
		40.605	2.2200	2.1975	Hex.Bi_2Te_3	(110)	14.4	

The surface morphology of $Bi_xSb_{2-x}Te_3$ thin films which deposited on glass substrate at room temperature with different Bi percentage of (x) where (x=0, 0.1, 0.3, 0.5, and 2), and different thickness (100, 300 and 500 nm), which involving the average grain size and surface roughness, as shown in Figs.5-7. The average grain size of $Bi_x Sb_{2-x}Te_3$ thin films decreases with increasing of the Bi percentage, as shown in Table 4, which involving the information about this analysis. The grain size is((95.31 nm) when x=0 and it decreases to (73.68 nm) when x=2 for thickness 100nm), also the grain size is (105.13 nm) when x=0 and it decreases to (76.52 nm) when x=2 for thickness 300 nm), while thickness (500 nm) the grain size is (108.85 nm) when x=0 which it decreases to (91.60 nm) when x=2. This may be seamed with the changing in atomic radius, and these results are agreed with those results which get from XRD analysis and also agree with Inad [21]. Also its observed that there is decreasing in surface roughness with increasing of Bi percentage, from

(0.755) nm at x=0 to (0.682) nm at x= 2 for the thickness 100nm, and from (1.56 nm) at x=0 to (1.41 nm) at x=2 for thickness 300 nm), while for thickness 500 nm the roughness decreases from (1.62 nm) at x=0 to (1.20 nm) at x=2. These results agree with Takashiri et al. [22].

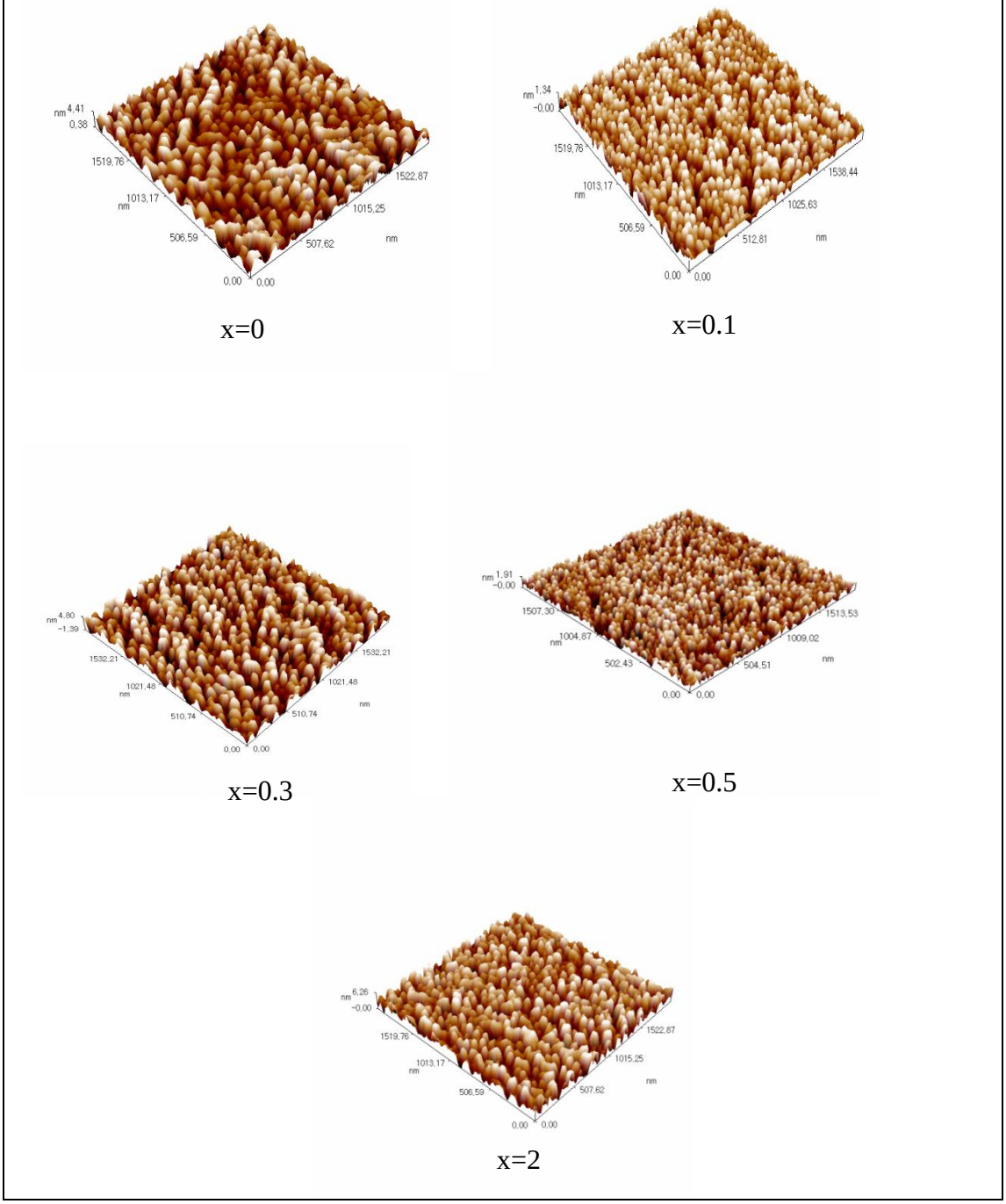

Fig.5: AFM images for $Bi_xSb_{2-x}Te_3$ thin films at thickness (100 nm).

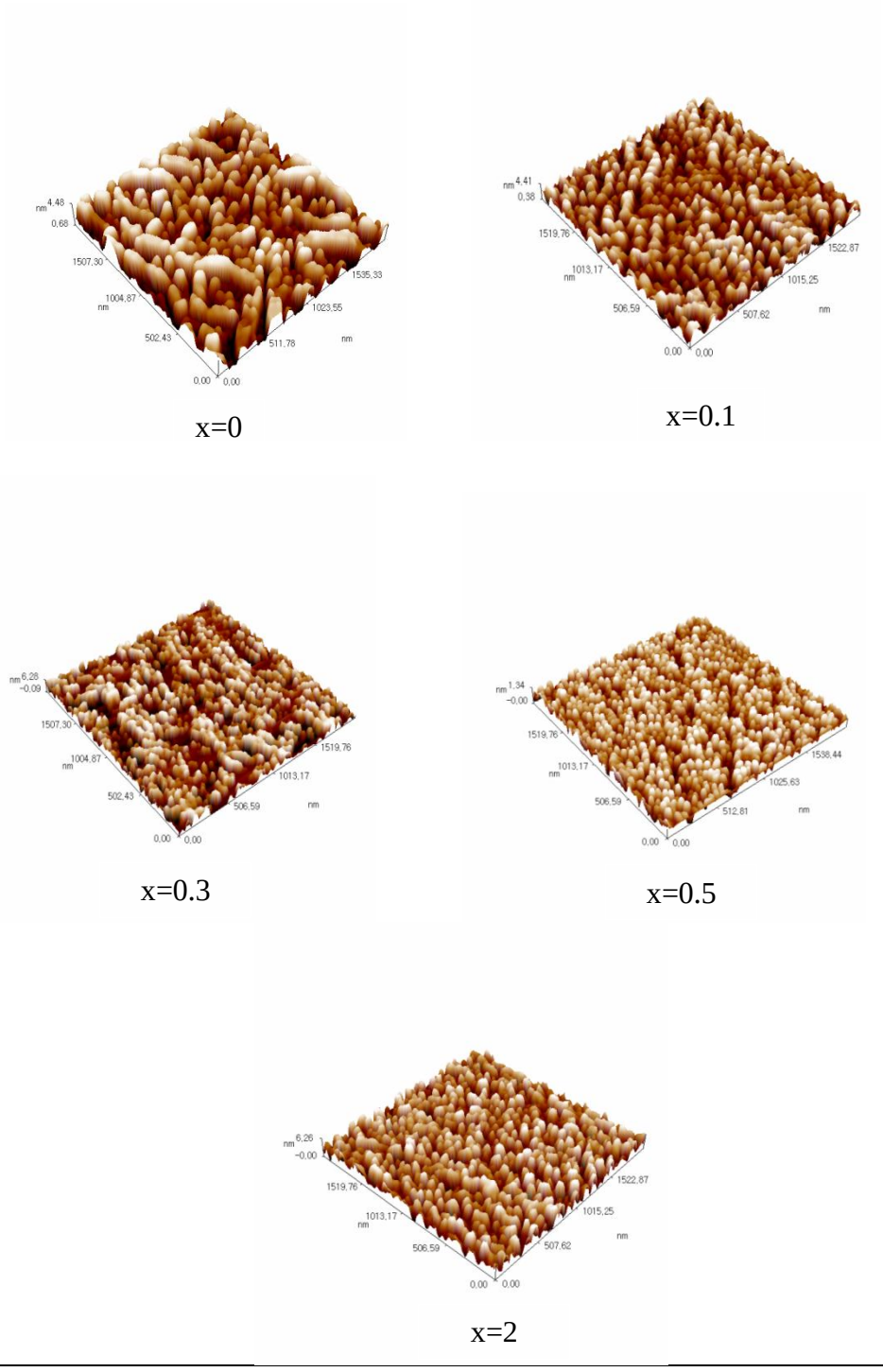

Fig.6: AFM images for $Bi_xSb_{2-x}Te_3$ thin films at thickness (300 nm).

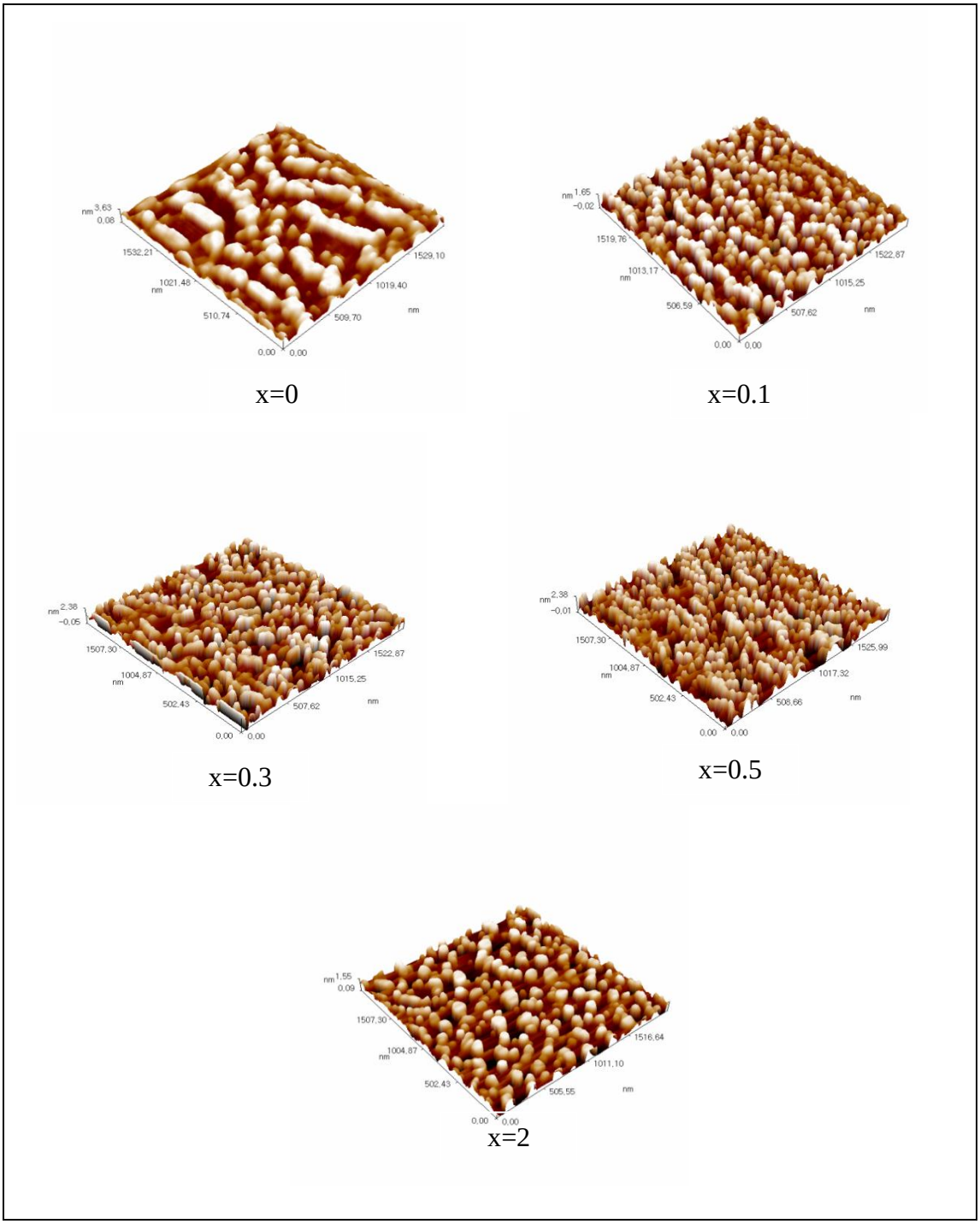

Fig.7: AFM images for $Bi_xSb_{2-x}Te_3$ thin films at thickness (500 nm).

Table 4: The average grain size and roughness for Bi_2 Sb_{2-x} Te_3 thin films deposited at room temperature with deferent zBi percentage (x=0, 0.1, 0.3, 0.5, and 2) and different thickness (100 nm, 300 nm, and 500 nm).

Thickness T(nm)	X	G.S (nm)	Roughness
100	0	95.31	0.755
	0.1	60.84	0.606
	0.3	55.70	0.575
	0.5	42.87	0.397
	2	73.68	0.682
300	0	105.13	1.56
	0.1	82.64	0.785
	0.3	63.80	0.476
	0.5	61.23	0.373
	2	76.52	1.41
500	0	108.85	1.62
	0.1	81.56	0.952
	0.3	76.02	0.906
	0.5	70.89	0.527
	2	91.60	1.20

Conclusions

The study of structural properties for $Bi_xSb_{2-x}Te_3$ thin films with different Bi percentage (0, 0.1, 0.3, 0.5, and 2), and different thickness (100 nm, 300 nm, and 500 nm) which deposited by thermal evaporation technique at R.T. was concluded:

1-All thin films have a polycrystalline structure with main peak (015), which move toward the smaller 2Θ.

2-The grain size of Bi_x $Sb_{2-x}Te_3$ thin films decreases with increasing of the Bi percentage for all thickness.

3-For the surface morphology of Bi_x $Sb_{2-x}Te_3$ thin films, the average grain size of $Bi_xSb_{2-x}Te_3$ thin films decreases with increasing of the Bi percentage.

References

[1] Rowe, D. M., in CRC Handbook of Thermoelectrics, Boca Raton, 90, (1995).

[2] D. Arivouli, F. D. Gnanam, P. Ramasamy, Mater J., 7 (1988) 711-713.

[3] S. M. Elahi, A. Taghizadeh, A. Hadizadeh L. Dejam, International Journal of Thin Films Science and Technology, 3, 1 (2014) 13-18.

[4] M.Z. Hasan, C.L. Kane, Rev. Mod. Phys., 82, 4 (2010) 3045-3067.

[5] R. Yu, W. Zhang, H.J. Zhang, S.C. Zhang, X. Dai, Z. Fang, Science, 329 (2010) 61-64.

[6] D. R. Lovett, Pion Limited, London, (1977) 181-197.

[7] P.G. Ganesan and V. Damodara Das, Mater. Lett., 60 (2006) 2059-2065.
[8] P.P. Pradyumnan and S. Wathikrishnan, University of Calicut, Calicut, India, (2010).
[9] Joy Kumar Das and M. A. I. Nahid, Int. J. Thin. Fil. Sci. Tec., 4, 1 (2015) 1-5.
[10] A. M. Adam, P. Petkov, M. El-Khouly, International Journal of Advances in Science Engineering and Technology, 6, 2 (2018) 46-52.
[11] C. Kittel, "Introduction to solid state physics", John Wiley and sons, 5th edition, (1986).
[12] J.V. Gilfrich, I.C. Noyan, R. Jenkins, T.C. Huang, R.L. Snyder, D.K. Smith, M.A. Zaitz, P.K. Predecki, "Advances in X – Ray Analysis", Springer US, Vol. 39, (2004).
[13] S. L. Solymar, D. Walsh, "Electrical Properties of Materials", Oxford, New York, Tokoy, (1998).
[14] A. Beiser, "Concepts of Modern Physics", McGraw-Hill Kogakusha, LTD, 2nd Edition, (1980).
[15] A.Islam, M.Islam , M. Choudhury and M.Hossan, "Recent Development in Condenced Matter Physics and Nuclear Science", Rajshahi University, Bangladesh, (1998).
[16] Ming Tan, Yanming Hao, Yuan Deng, Dali Yan, Zehua Wu, Scientific Reports, 8 (2018) 1-9.
[17] F. S.Sánchez, M. Gharsallah, N. M. Nemes, N. Biskup, M. Varela, J. L.Martíne, M. T. F. Díaz, J. A. Alonso, Scientific Reports, 7, 1 (2017) 1-10.
[18] C. Zhang, Z. Peng, Z. Li, L. Yu, K.A. Khor, Q. Xiong, Nano Energy, 15 (2015) 688-696.
[19] Junqiang Song, Qin Yao, Ting Wu, Xun Shi, Lidong Chen, Electron. Mater. Lett., 9, 6 (2013) 709-713.
[20] J. K. Das and M.A.I. Nahid, International Journal of Thin Films Science and Technology, 4, 1 (2015) 13-16.
[21] Khalil Ibrahim Inad, "Study thermoelectrical characterization (Bi_2Te_3), $(Bi_2Te_3)_xSb_{1-x}$ and $(Bi_2Te_3)_xSe_{1-x}$ as a Peltier device", Baghdad University, PhD thesis (2014).
[22] M.Takashiri, K. Miyazaki, H. Tsukamoto, Electrodepositing Journal of Applied Electrochemistry, 33 (2003) 23-27.